

AD-A268 503



INATION PAGE

Form Approved
OBM No. 0704-0188



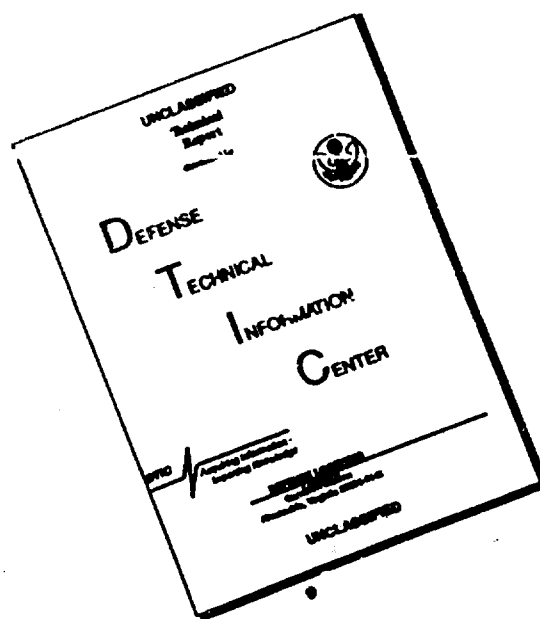
page 1 hour per response, including the time for reviewing instructions, searching existing data sources, gathering and
rmaton. Send comments regarding this burden or any other aspect of this collection of information, including suggestions
or Information Operations and Reports, 1215 Jefferson Davis Highway, Suite 1204, Arlington, VA 22202-4302, and to
1189), Washington, DC 20503.

1. Agency Use Only (Leave blank).		2. Report Date. October 1992		3. Report Type and Dates Covered. Final - Proceedings	
4. Title and Subtitle. Vertical and Horizontal Heat Transfer from A Limited-Area Heat Source				5. Funding Numbers. Contract Program Element No. 0601153N Project No. Task Accession No. DN252020 Work Unit No. 14422A	
6. Author(s). John W. Glendening					
7. Performing Organization Name(s) and Address(es). Naval Research Laboratory Marine Meteorology Division Monterey, CA 93943-5006					
9. Sponsoring/Monitoring Agency Name(s) and Address(es). Naval Research Laboratory Marine Meteorology Division Monterey, CA 93943-5006				8. Performing Organization Report Number. PR 92:102:441	
10. Sponsoring Monitoring Agency Report Number. PR 92:102:441				11. Supplementary Notes. Published in Tenth Symposium on Turbulence and Diffusion.	
12a. Distribution/Availability Statement. Approved for public release; distribution is unlimited.				12b. Distribution Code.	
13. Abstract (Maximum 200 words). This paper investigates the heat budgets produced by a limited area heat source, as modelled in a large-eddy simulation. The physical prototype is a series of Arctic leads, breaks in the Arctic pack ice which allow relatively warm ocean water to contact the cold atmosphere. This idealized case represents periodic inhomogeneous surface conditions. Local budgets of temperature and vertical turbulent heat flux will be compared to their domain averaged values.					
14. Subject Terms. Air-sea interaction, boundary layer, coupled models				15. Number of Pages. 4	
17. Security Classification of Report. Unclassified				18. Security Classification of This Page. Unclassified	
19. Security Classification of Abstract. Unclassified		20. Limitation of Abstract. SAR			

424
77i
93-19020

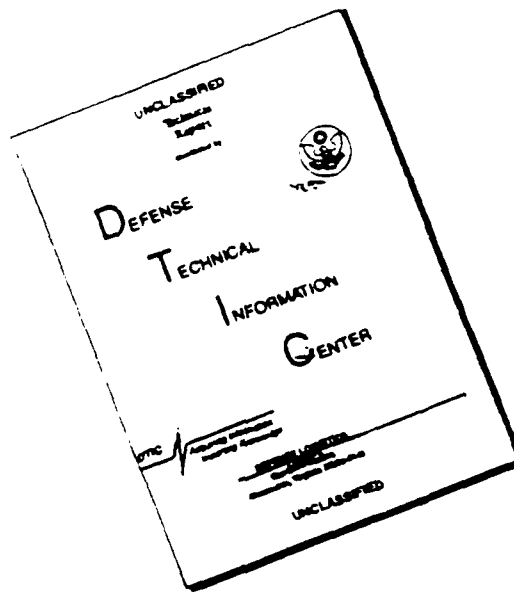


DISCLAIMER NOTICE



THIS DOCUMENT IS BEST QUALITY AVAILABLE. THE COPY FURNISHED TO DTIC CONTAINED A SIGNIFICANT NUMBER OF PAGES WHICH DO NOT REPRODUCE LEGIBLY.

DISCLAIMER NOTICE



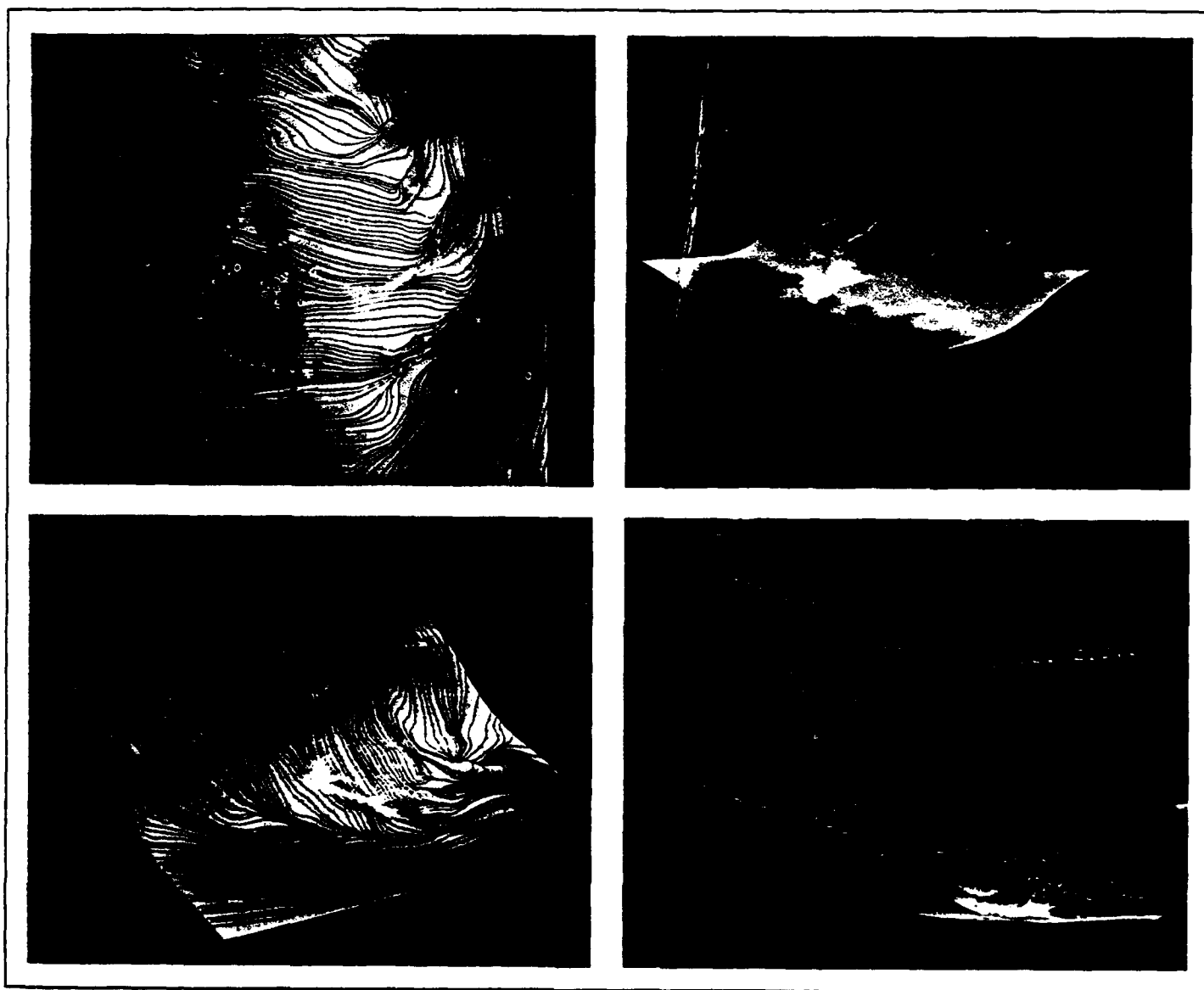
THIS DOCUMENT IS BEST
QUALITY AVAILABLE. THE COPY
FURNISHED TO DTIC CONTAINED
A SIGNIFICANT NUMBER OF
PAGES WHICH DO NOT
REPRODUCE LEGIBLY.

Preprints

TENTH SYMPOSIUM ON TURBULENCE AND DIFFUSION

29 Sept-2 Oct 1992

Portland, Oregon



AMERICAN METEOROLOGICAL SOCIETY

VERTICAL AND HORIZONTAL HEAT TRANSFER FROM A LIMITED-AREA HEAT SOURCE

John W. Glendening

Naval Research Laboratory Monterey
Monterey, California

1. INTRODUCTION

This paper investigates the heat budgets produced by a limited area heat source, as modelled in a large-eddy simulation. The physical prototype is a series of Arctic leads, breaks in the Arctic pack ice which allow relatively warm ocean water to contact the cold atmosphere. This idealized case represents periodic inhomogeneous surface conditions. Local budgets of temperature and vertical turbulent heat flux will be compared to their domain averaged values.

2. LARGE-EDDY SIMULATION

A previous large-eddy simulation which modelled a single lead, by not allowing a parcel to cycle through the domain (Glendening and Burk, 1992), has been extended for approximately three parcel cycles with periodic lateral boundary conditions, representing periodic surface forcing as might occur over multiple leads.

Idealized initial conditions consist of a air-water temperature difference of 25K over a 200m wide lead, below a linear stratification of $\partial\theta/\partial z = 10\text{K/km}$. The large-scale geostrophic wind speed is 2.5m/s perpendicular to the lead edge. These conditions generate a large surface temperature flux over the lead, averaging 0.162K/s. Over the surrounding ice the surface temperature flux is downward, due to the warmer air above it, averaging -0.0076K/s. The heat source covers only 9% of the domain, so the domain averaged temperature flux is +0.0071K/s.

The large-eddy model used is fundamentally that described in Moeng (1984), except that surface inhomogeneity is introduced, a radiative boundary condition is employed at the model top, the mixing length is required to meet similarity restrictions near the surface, and the surface similarity includes stable conditions. Further details are given in Glendening and Burk (1992). This simulation requires much smaller grid spacing than that of a convective boundary-layer (BL). Vertical resolution is 4m and horizontal resolution is 8m. The grid covers 2304m perpendicular to the lead, 192m transversely, and 120m vertically (x, y, z directions respectively). The time step is 0.5s. Local averaging, both in time and parallel to the lead, is required to obtain adequate statistics; the results presented are for $t=0.6-0.7\text{hr}$, so local averages are based upon 17,280 values.

3. LOCAL AVERAGES

Fig. 1 gives contours of potential temperature $\bar{\theta}$, where the overbar represents a local average. The stable

stratification established upwind of the lead is eroded by the turbulence created by the warm surface, producing a relatively well-mixed region. Below this region a stable internal boundary layer grows downwind of the lead. The figure does not cover the entire horizontal domain, so differences between the left and right borders represent the increasing stratification which results further downwind.

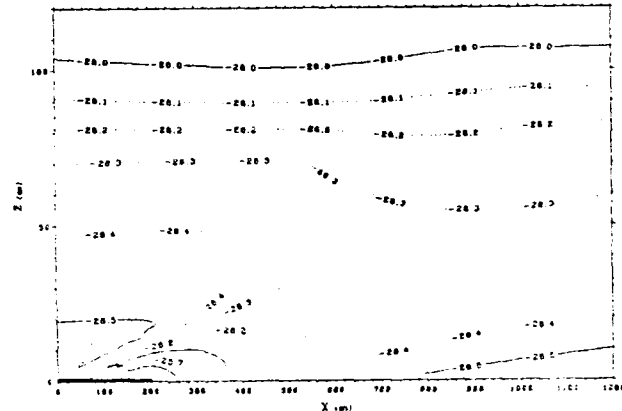


FIG. 1: Potential temperature $\bar{\theta}$ (in $^{\circ}\text{C}$).

Because much of the domain is stably stratified, the "large-eddy" results apply only to the region of the grid within which turbulence is resolved. Fig. 2, giving contours of w'^2 where ' represents a deviation from the local average, indicates that region. For a parcel, travel time over the lead is relatively short --compared to the Brunt-Väisälä period-- so the maximum vertical velocity of an individual thermal occurs considerably downwind of the lead. Here I use "thermal" to indicate an individual eddy, whose combined effects produce the "plume" apparent in Fig. 2. Note that the downwind tilt of the plume signifies that an individual thermal which reaches its maximum vertical velocity later/sooner than the "typical" thermal is usually both further/closer downwind and further/closer from the ground; this tilt does not characterize the individual thermals, which are essentially vertically oriented.

Fig. 3 displays the total vertical turbulent temperature flux, summing the resolved and unresolved contributions. The upward flux is strongest at the surface, with a maximum axis tilting downwind. The heat plume downwind of the lead results from the net heat carried by individual thermals. Downward heat flux occurs in the downwind portion of the plume and also at the surface.

NTIS CRA&I	<input checked="" type="checkbox"/>
DTIC TAB	<input type="checkbox"/>
Unannounced	<input type="checkbox"/>
Justification	

By _____
Distribution /

Availability Codes

Dist Avail for

DTIC QUALITY INSPECTED 39-1 20

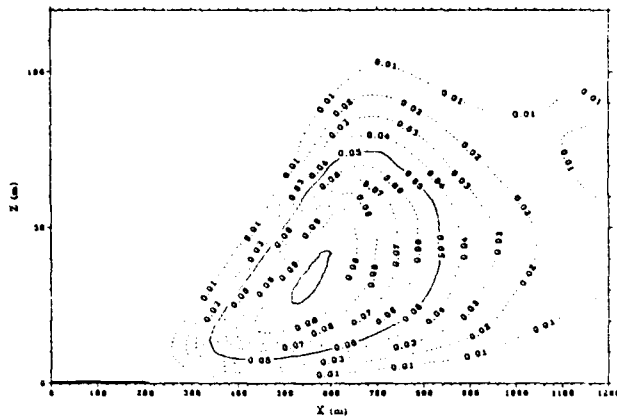


FIG. 2: Resolved vertical turbulence $\overline{w''^2}$ (in m^2/s^2).

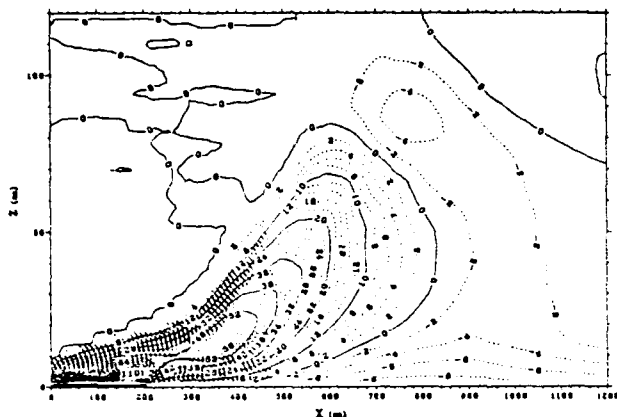


FIG. 3: Total vertical turbulent temperature flux (in $x10^3 Km/s$).

Although not shown, the profile of $\overline{w''^2}$, where " represents a deviation from the domain average ($\overline{\quad}$), is both qualitatively and quantitatively similar to that expected for a convective BL over a homogeneous surface, when non-dimensionalized by $w_* \equiv [gQ_s D / \theta_s]^{1/3}$ where Q_s is the domain averaged surface temperature flux and D is the plume depth as defined by the level of maximum domain-averaged downward turbulent heat flux. Non-dimensionalization of this inhomogeneous case using homogeneous convective BL scaling based upon domain means is thus appropriate, despite the large horizontal inhomogeneities and the limited region of strong turbulence downwind of the unstable surface. This non-dimensionalization, which will be called "periodic" scaling to emphasize its employment under inhomogeneous conditions, allows comparison to results obtained for a horizontally homogeneous BL.

4. TEMPERATURE BUDGETS

Fig. 4 presents dimensional profiles of domain averaged vertical temperature flux. The total flux profile is qualitatively similar to that over a homogeneous heated surface, but here the linear decrease with height does not indicate a well-mixed region, since such is not found in the domain mean temperature profile, but simply that the shape of the temperature profile remains constant with time. As would occur for homogeneous surface heating, there is a net downward heat flux near the top

of the plume region, but its magnitude is smaller than expected for a homogeneous convective BL. Only a minor portion of the vertical heat transport occurs through mean motion, a consequence of mean vertical velocities being relatively small. Note that the vertical turbulent flux based upon perturbations from the domain mean is simply the sum of the local mean and turbulent fluxes, i.e. $\overline{w''\theta''} = \overline{w''\theta} + \overline{w'\theta'}$. Fig. 5 presents the domain averaged $\partial\overline{\theta}/\partial t$ budget, non-dimensionalized by the periodic scaling Q_s/D , for comparison to local $\partial\theta/\partial t$ budgets presented below.

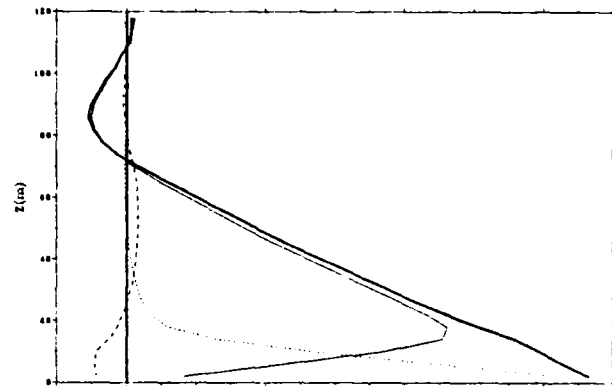


FIG. 4: Domain average of vertical temperature flux (in $x10^3 Km/s$): mean $\overline{w\theta}$ (dashes), turbulent $\overline{w'\theta'}$ (thin solid), subgrid (dots), and total (thick solid).

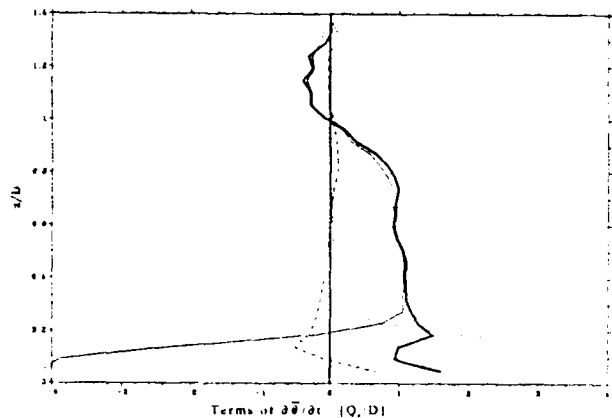


FIG. 5: Non-dimensional domain average of $\partial\overline{\theta}/\partial t$ budget terms: mean vertical flux $-\partial\overline{w\theta}/\partial z$ (dashes), turbulent vertical flux $-\partial\overline{w'\theta'}/\partial z$ (thin solid), subgrid (dots), and total (thick solid).

Fig. 6 presents local profiles at three locations, spaced equally about the position of maximum plume growth: upwind ($x=400m$), at ($x=600m$), and downwind ($x=800m$). All perturbations are based upon deviations from the local average, not from the domain mean average.

Upwind of the position of maximum plume growth (Fig. 6a), vertical turbulent flux creates cooling at the surface, which is countered by horizontal transport of warm air immediately above the lead. Turbulent heating occurs above this, through a depth about equal to that of the lower region, and is countered by a mean horizontal flux which is now relatively cool. The remaining terms are relatively small in magnitude. The net $\partial\theta/\partial t$ has a warming maximum at $0.4D$.

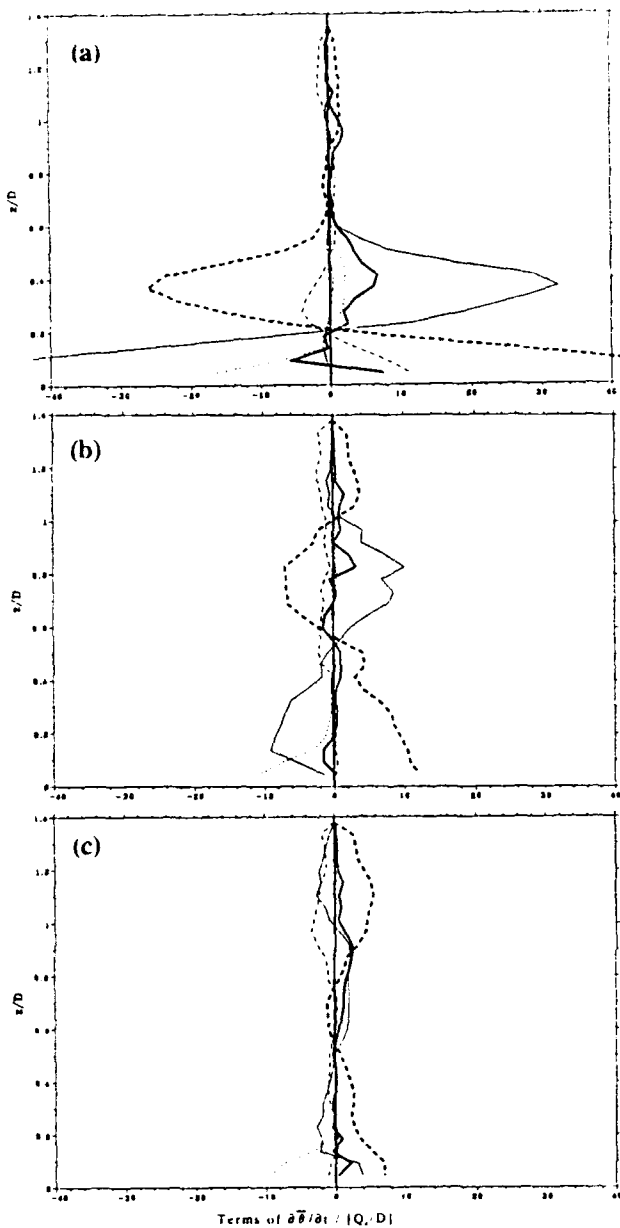


FIG. 6: Non-dimensional $\partial \bar{\theta} / \partial t$ budget terms at: (a) $x=400m$ (b) $x=600m$ (c) $x=800m$. Symbols as for Fig. 5 plus mean horizontal flux $-\partial \bar{u} \bar{\theta} / \partial x$ (thick dash) and turbulent horizontal flux $-\partial \bar{u}' \bar{\theta}' / \partial x$ (dash-dot).

At the position of maximum plume growth (Fig. 6b), results are qualitatively similar to those upwind but are smaller quantitatively and, in addition, cooling resulting from mean vertical transport is opposed by heating from horizontal mean transport, resulting from the upward tilt of the isentropes.

Downwind of the position of maximum plume growth (Fig. 6c), the terms are further reduced in magnitude. The primary qualitative difference from the previous locations is the additional cooling just above D resulting from downward turbulent transport, which helps counter the warming horizontal transport. The net warming $\partial \bar{\theta} / \partial t$ now occurs at a higher level than at upwind positions.

Locally, therefore, mean horizontal transport is of major importance. The sign of the horizontal transport changes with height --warming near the surface, cooling

above, and then warming near the plume top-- and opposes the effect of vertical turbulent transport. The net horizontal turbulent transport is negligible at all locations, although it can be significant for an individual eddy. For the domain average of the local terms (Fig. 5), the horizontal transport terms must sum to zero due to the lateral periodicity.

5. VERTICAL TURBULENT HEAT FLUX BUDGETS

Fig. 7 presents domain averages of the terms of the local $\partial \bar{w}' \bar{\theta}' / \partial t$ budget, non-dimensionalized by the periodic scaling $w_e Q_e / D$, for comparison to the local budgets presented below. These profiles are not equivalent to the corresponding terms from domain budgets of $\partial \bar{w}'' \bar{\theta}'' / \partial t$, but are generally similar in form since mean vertical motion is small and local averages usually not too different from the domain averages. The primary difference of the $\partial \bar{w}'' \bar{\theta}'' / \partial t$ budget lies in its buoyant and pressure terms, which become increasingly larger near the surface.

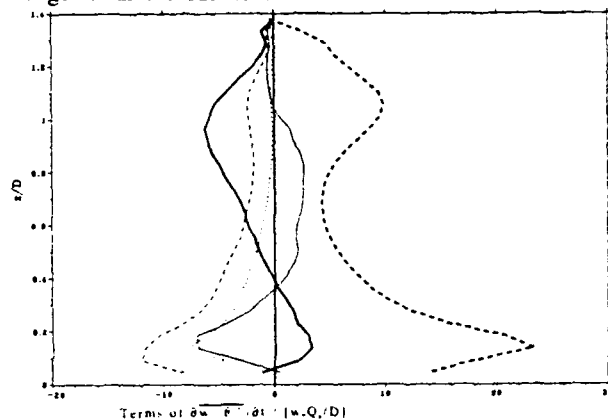


FIG. 7: Non-dimensional domain average of $\partial \bar{w}' \bar{\theta}' / \partial t$ budget terms: vertical temperature gradient $-\bar{w}' \bar{w}' \partial \bar{\theta}' / \partial z$ (thick solid), vertical turbulent transport $-\partial \bar{w}' \bar{w}' \bar{\theta}' / \partial x$ (solid), buoyant $g \bar{\theta}' \bar{\theta}' / \Theta_e$ (thick dashes), pressure correlation $-\bar{\rho}' \bar{\theta}' \partial \bar{p}' / \partial z$ (dashes), and subgrid (dots).

The profiles in Fig. 7 are similar, both qualitatively and quantitatively, to those obtained over a homogeneous surface except that the gradient production term is significantly larger above the mid-plume level. Buoyant production is positive with maxima at the ground and near D. Its maximum at D is of smaller magnitude than that of a homogeneous BL. Buoyant production is balanced primarily by pressure correlation only in the lower plume, gradient production being more significant in the upper plume. Turbulent transport exports heat flux from the lower to upper plume. Vertically integrated gradient production is negative, due to the stratification into which the plume must grow.

Fig. 8 presents local $\partial \bar{w}' \bar{\theta}' / \partial t$ budgets at the three locations used for the temperature budgets, for comparison with the domain averages of Fig. 7. Several terms of a horizontally inhomogeneous heat budget have not been plotted because their contribution is relatively small.

Upwind of the position of maximum plume growth (Fig. 8a), buoyant production is the largest positive term, countered primarily by vertical turbulent transport.

Gradient production is a significant positive terms, not the negative term of the domain average. Pressure correlation counters positive turbulent transport in the upper portion of the turbulent region.

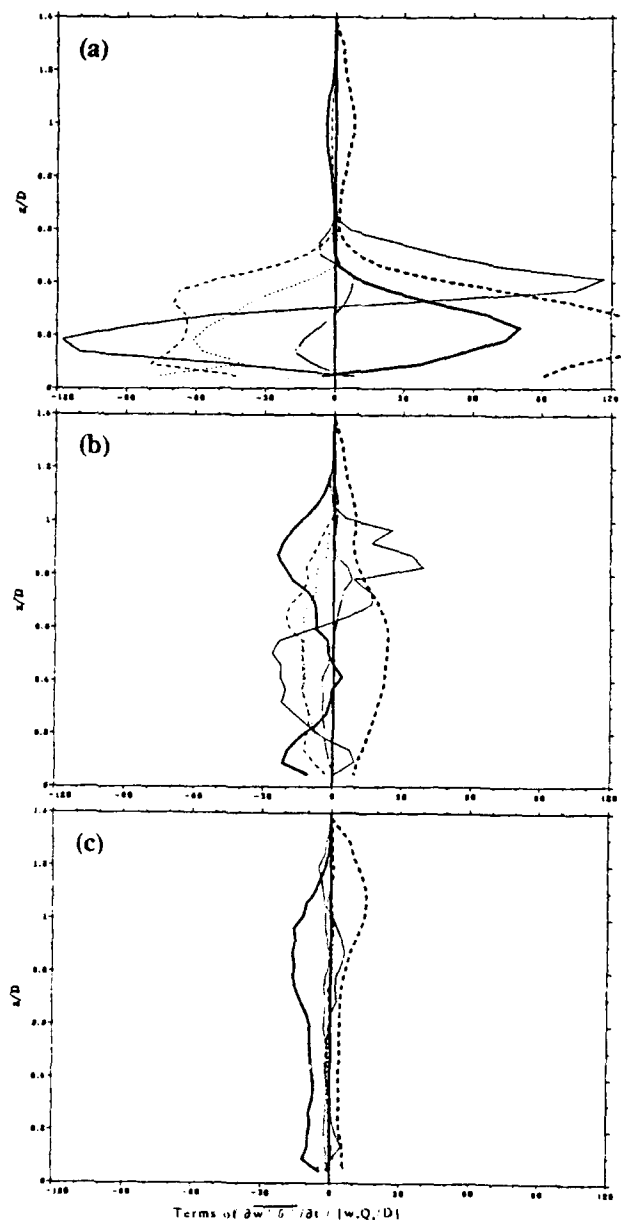


FIG. 8: Non-dimensional $\partial w' \theta' / \partial t$ budget terms at: (a) $x=400m$ (b) $x=600m$ (c) $x=800m$. Symbols as for Fig. 7 plus horizontal mean flux $-\partial u w' \theta' / \partial x$ (dash-dot).

At the position of maximum plume growth (Fig. 8b), the buoyant production maximum has moved upward and weakened, as have the maxima of positive and negative transport. Gradient production is now negative throughout the plume depth, reaching a maximum just below D. At most levels the negative pressure correlation makes only a secondary contribution.

Downwind of the position of maximum plume growth (Fig. 8c), buoyant production is still the primary positive term but its maximum lies just above D. The primary negative term is gradient production.

Overall, buoyant production is the primary positive budget term, its maximum moving upward and decreasing in magnitude downwind. Gradient production is initially positive, but quickly becomes a major negative term due to the stable stratification which the atmosphere seeks to establish. Unlike the temperature budget, the horizontal transport contribution to the $w' \theta'$ budget is small for the local budgets. The local terms sum to give the domain average effect, which is much smaller than local term values. Turbulent transport is strongest where w'^2 is largest, in the initial growth region of the plume. Near the plume top, gradient production --not pressure correlation-- is the primary negative term. The region downwind of the plume makes the largest contribution to downward $w' \theta'$.

6. CONCLUSIONS

The heat flux generated over a limited-area heat source is transported vertically by individual thermals to create a mean plume downwind. Domain averaged terms of $\partial \bar{\theta} / \partial t$ and $\partial \overline{w' \theta'} / \partial t$ (and $\partial w'' \theta'' / \partial t$) are generally similar to those over a homogeneous surface, qualitatively and quantitatively, when non-dimensionalized by periodic scaling. For the $\partial \overline{w' \theta'} / \partial t$ equation, however, gradient production is significantly larger than over a homogeneous surface, due to stable stratification surrounding the plume, and dominates the pressure correlation term near the plume top. For the local $\partial \bar{\theta} / \partial t$ equation, mean horizontal transport is of major importance.

The similarity of the domain averaged budget terms to those of a homogeneous convective BL depends upon mean transport being small; for simulations with larger mean vertical transport, as when the flow is more parallel to the lead and advection perpendicular to the plume decreases and departures occur. Thus the results presented here apply only when mean vertical motion is small.

There are many caveats for any simulation such as this. I believe that its most significant limitations are: (1) the results depend upon the chosen parameterization for the subgrid length scale, which especially affects the transition from resolved to unresolved turbulence at the plume edge, and (2) the horizontal resolution is twice the vertical resolution.

ACKNOWLEDGEMENTS

The support of the sponsor, Naval Oceanographic and Atmospheric Research Laboratory, Ms. H. Morris, Program Element 61153, is gratefully acknowledged (Contribution 92:102:441, approved for public release with unlimited distribution). I thank the Department of Meteorology and Computer Center of the Naval Postgraduate School for their support.

REFERENCES

- Glendening, J.W. and S.D. Burk. 1992: Turbulent transport from an Arctic lead: a large-eddy simulation. *Bound.-Layer Meteor.*, 59, 315-339.
- Moeng, C.-H., 1984: A large-eddy simulation model for the study of planetary boundary-layer turbulence. *J. Atmos. Sci.*, 41, 2052-2062.